A computational elucidation of the Structure-Property Relationships in Graphene-Organic 2D Crystal Heterostructures

Shuangjie Zhao[1], Miroslav Položij[1,2,3], Thomas Heine*[1,2,3,4]

[1]Chair of Theoretical Chemistry, Technische Universität Dresden, Bergstr. 66, 01069 Dresden, Germany

[2]Helmholtz-Zentrum Dresden-Rossendorf, HZDR, Bautzner Landstr. 400, 01328, Dresden, Germany

[3]Center for Advanced Systems Understanding, CASUS, Untermarkt 20, 02826 Görlitz, Germany

[4]Department of Chemistry and ibs for Nanomedicine, Yonsei University, Seodaemungu, Seoul 120-749, Republic of Korea

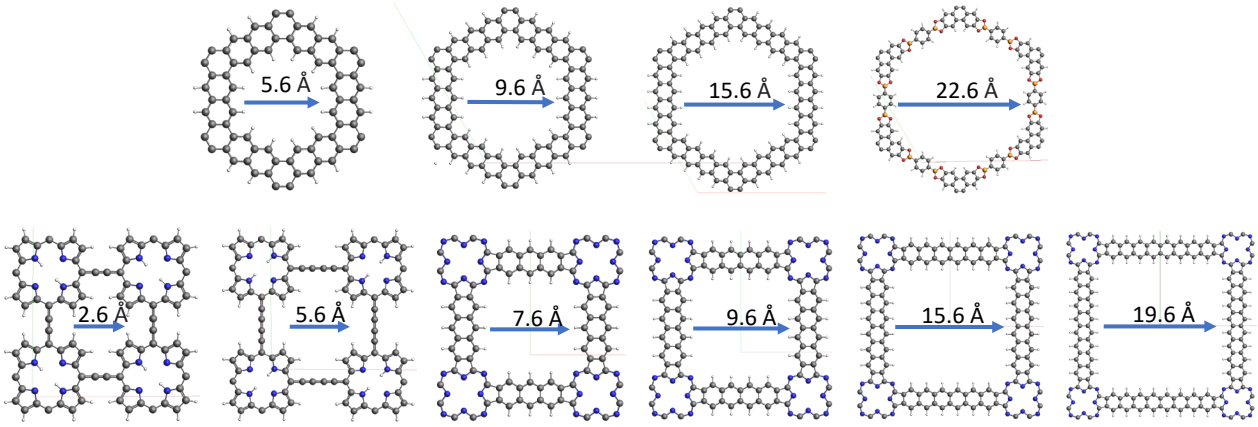

Figure S1. Ball-and-stick representations for structures of studied O2DCs (hcb: h1 to h4; sq: s1 to s6)

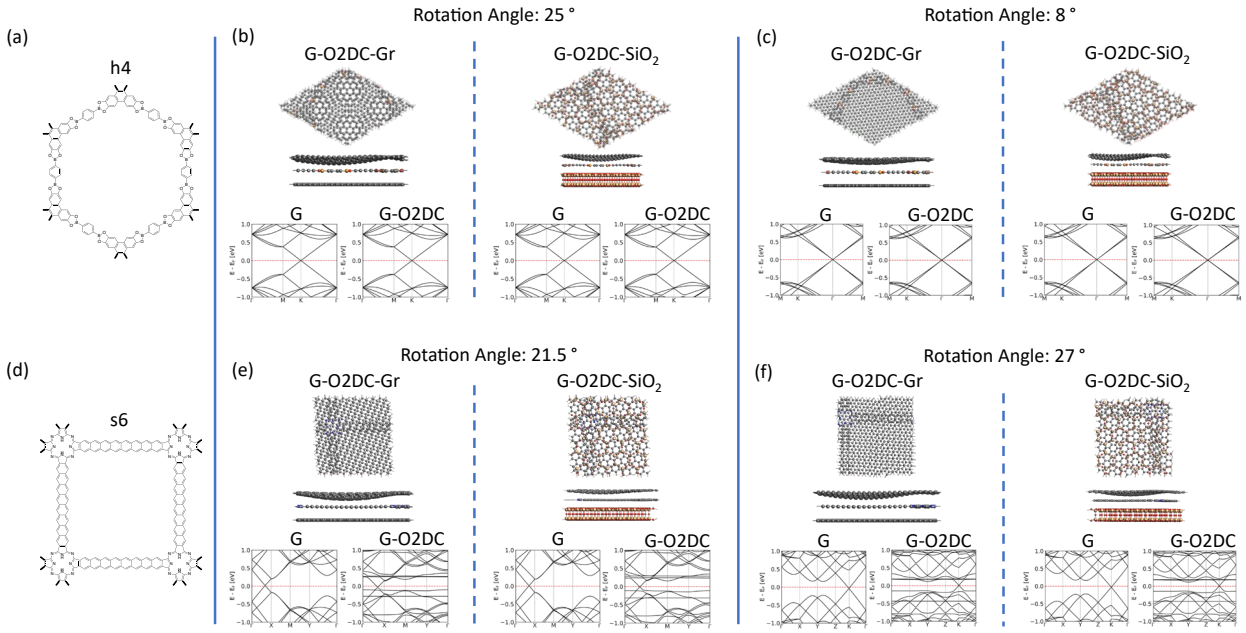

Figure S2. Band structures of G part only and G-O2DC part for G-O2DC-Gr and G-O2DC-SiO_2 structures of h4 (a) and s6 (d) with different rotational angle between G and O2DC layer. (25 ° and 8 ° for h4, 21.5 ° and 27 for s6).

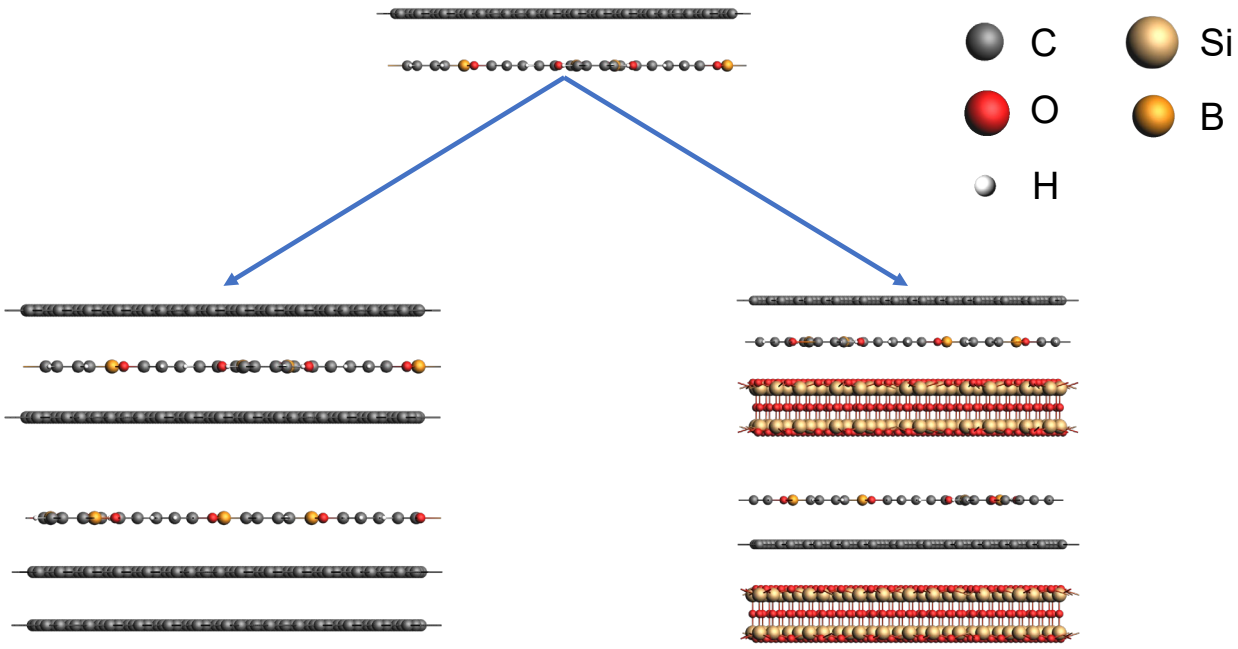

Figure S3. Ball-and-stick representation of investigated structures of h4 [1] as examples.

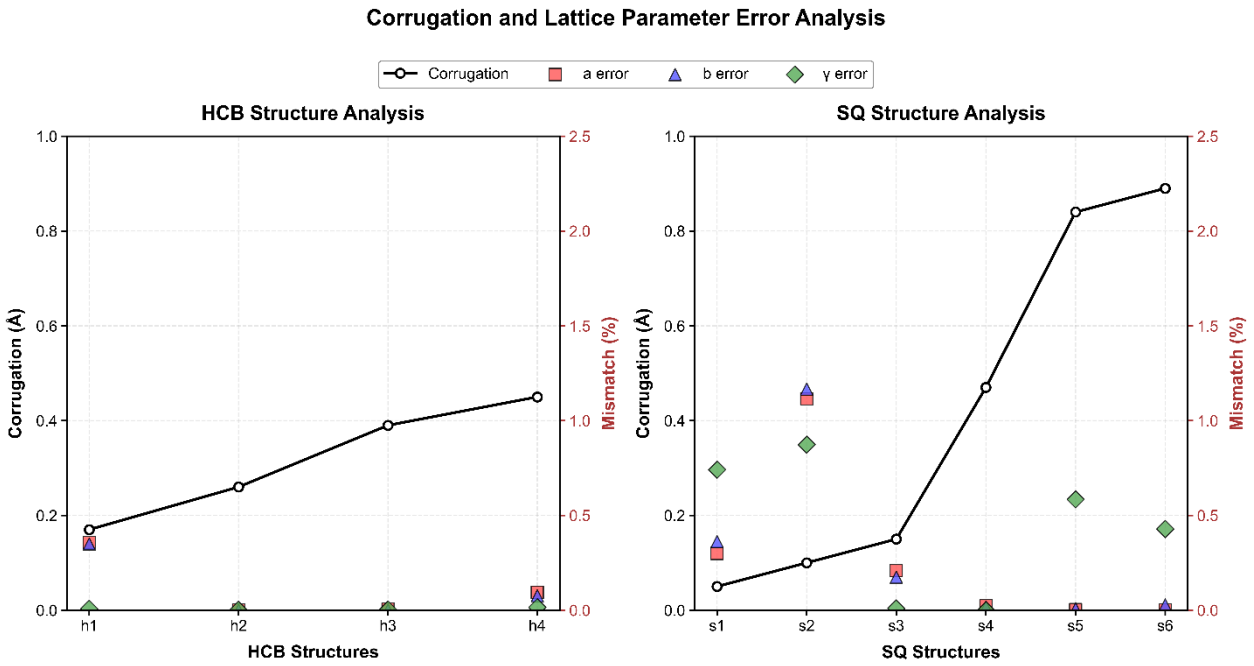

Figure S4. Analysis of lattice mismatch in built G-O2DC heterostructures (HCB: honeycomb; SQ: square). Lattice vector a, b and angle γ were compared between O2DCs alone and after being incorporated into heterostructures.

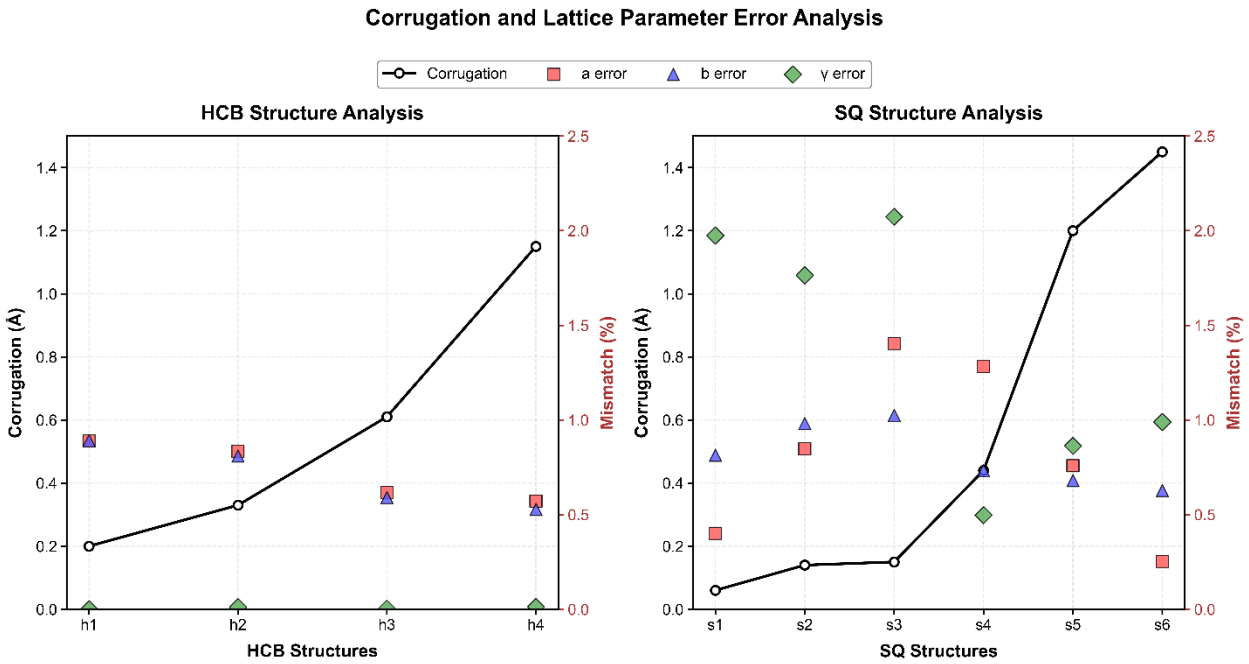

Figure S5. Corrugation in built G-O2DC-SiO_2 heterostructures (HCB: honeycomb; SQ: square) along with analysis of lattice mismatch.

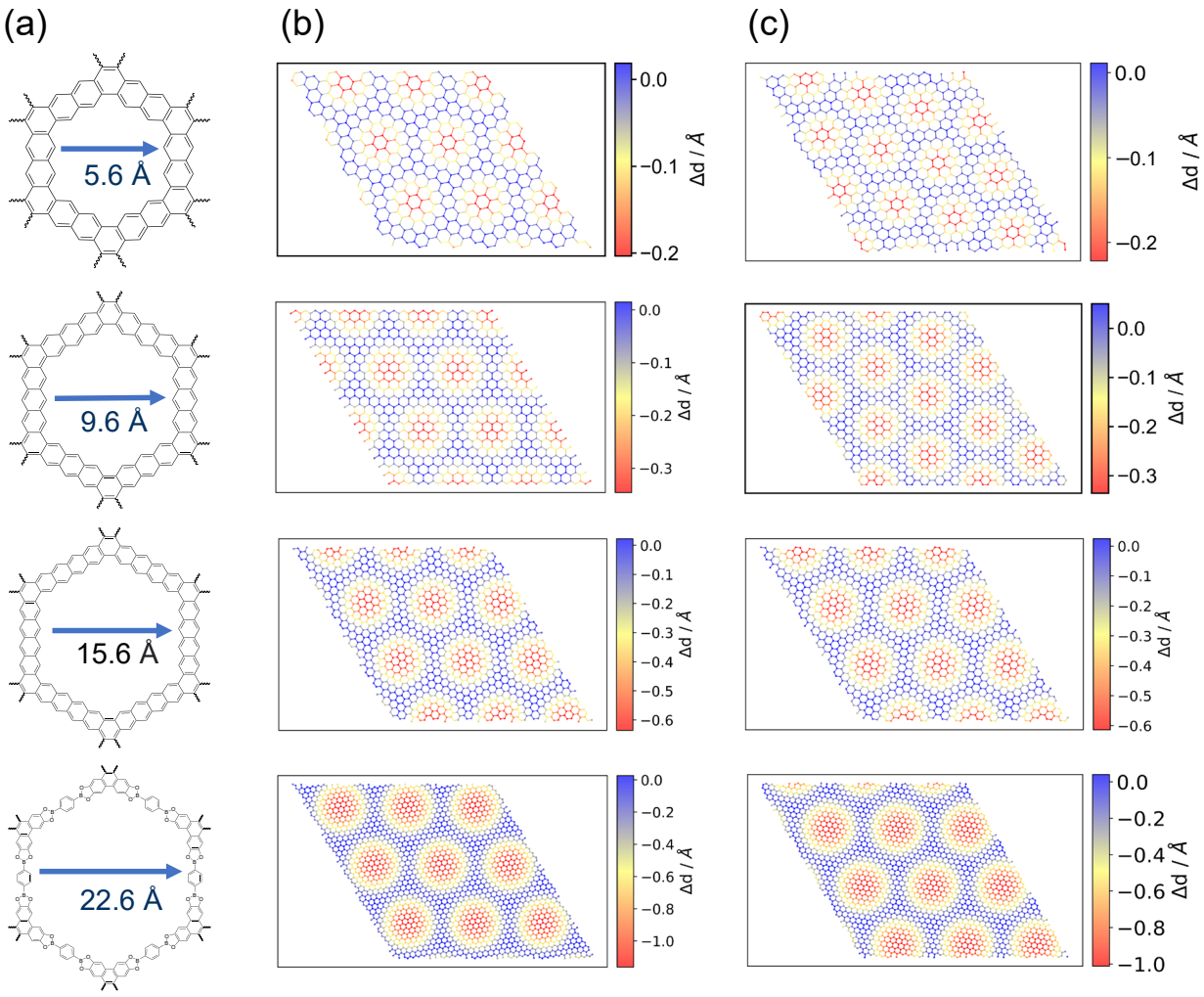

Figure S6. Full-spectrum deformation analysis of corrugation on graphene for G-O2DC-Gr (column b) and G-O2DC-SiO_2 (column c) structures for O2DC model h1 to h4. The rotational angles (RA) between G and O2DC are 18.9°, 0.0°, 23.0°, 8.0°, respectively.

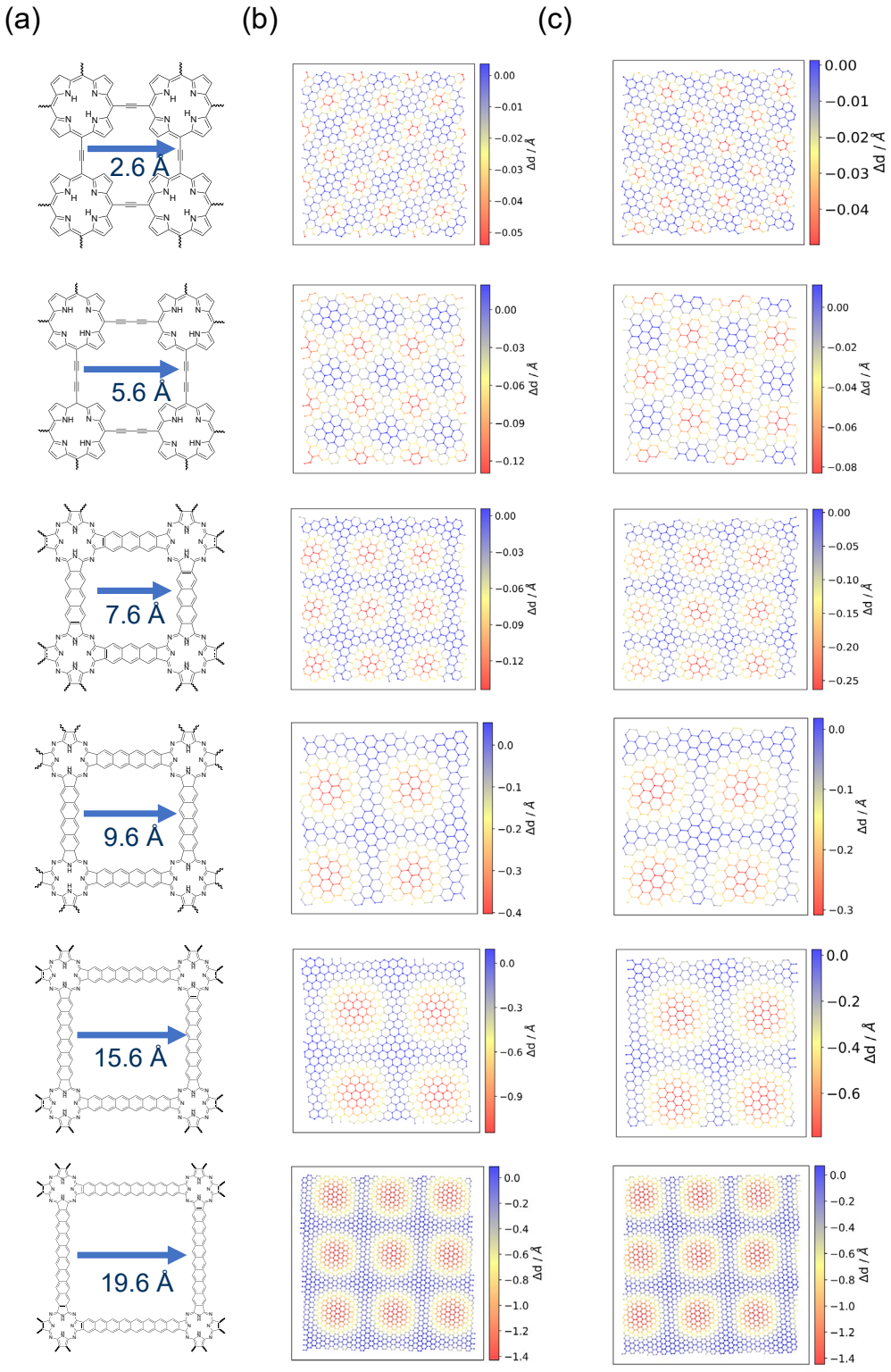

Figure S7. Full-spectrum deformation analysis of corrugation on graphene for G-O2DC-Gr (column b) and G-O2DC-SiO_2 (column c) structures for O2DC model s1 to s6. The rotational angles (RA) between G and O2DC are 0.0°, 9.9°, 13.8°, 5.5°, 34.2°, 27.0°, respectively.

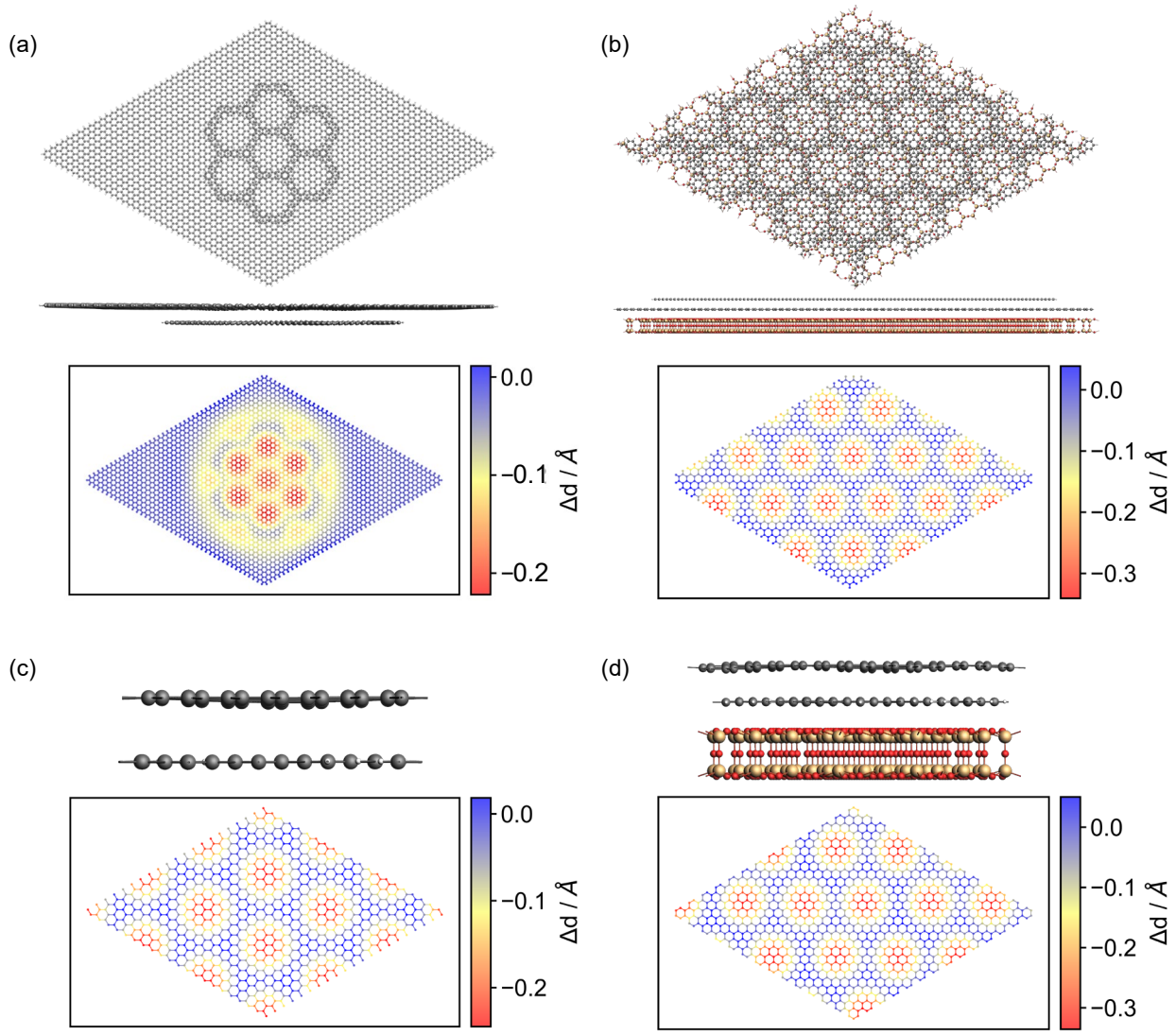

Figure S8. Test strategy and results of deformation analysis for strain in built non-periodic G-O2DC(h2) (a) and graphene flake on periodic O2DC(h2)-substrate (b, here substrate is SiO_2), and the comparison with the studied periodic G-O2DC(h2) structure (c) and G-O2DC(h2)-SiO_2 structure (d).

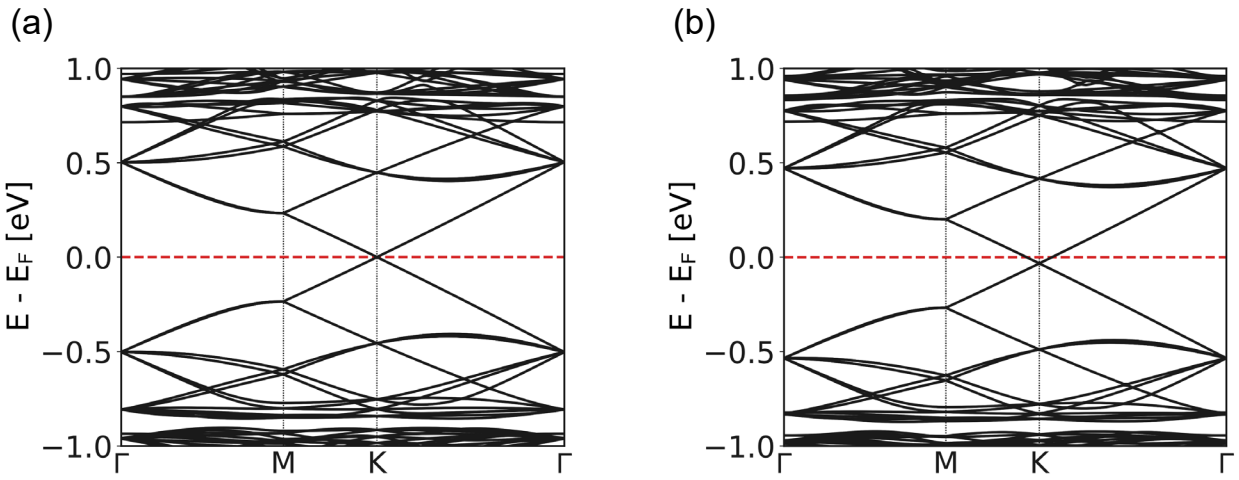

Figure S9. Band structures of G-O2DC(h1)-SiO_2 when SiO_2 was not (a) and was (b) included during only the band structure calculation.

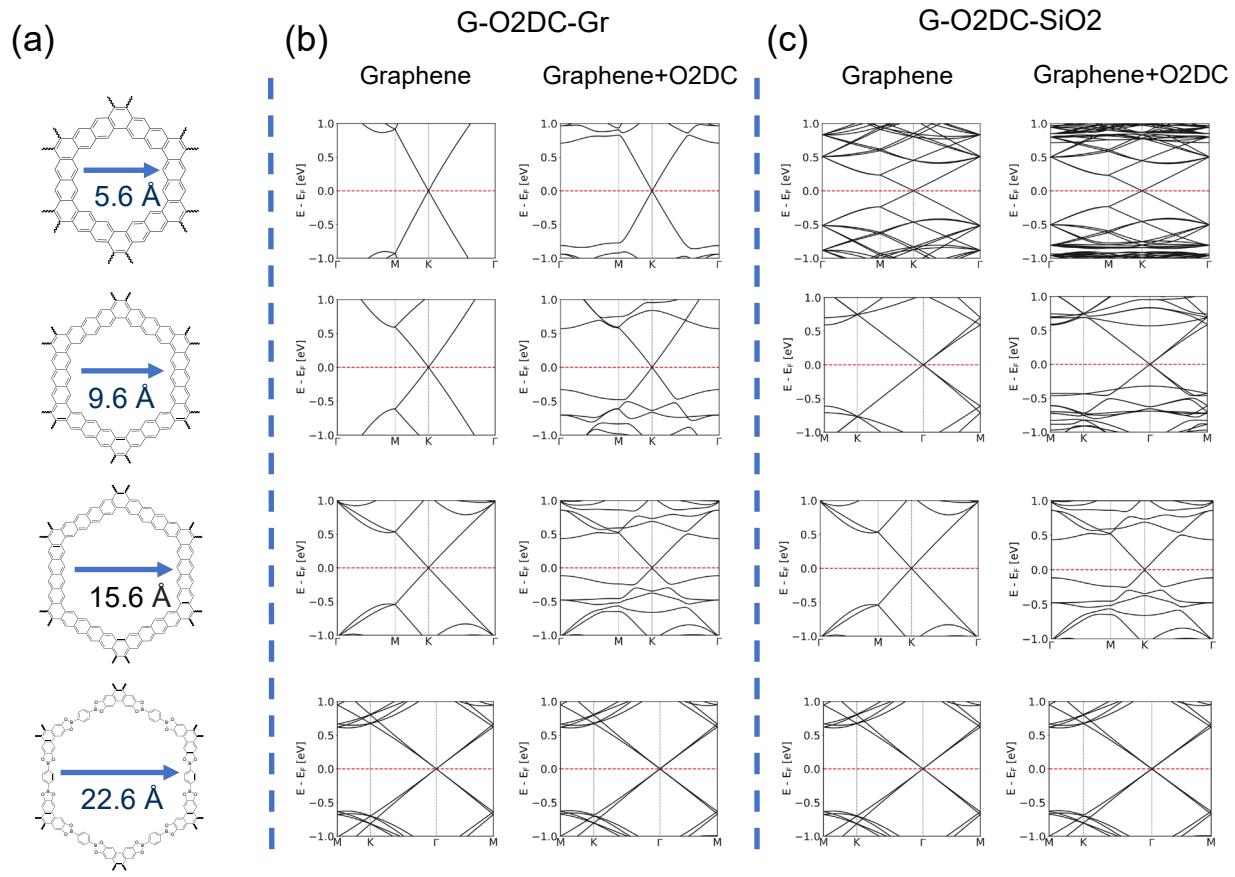

Figure S10. Band structures of sole graphene and graphene + O2DC moiety in G-O2DC-substrates (Gr and SiO_2) structures for h1 to h4.

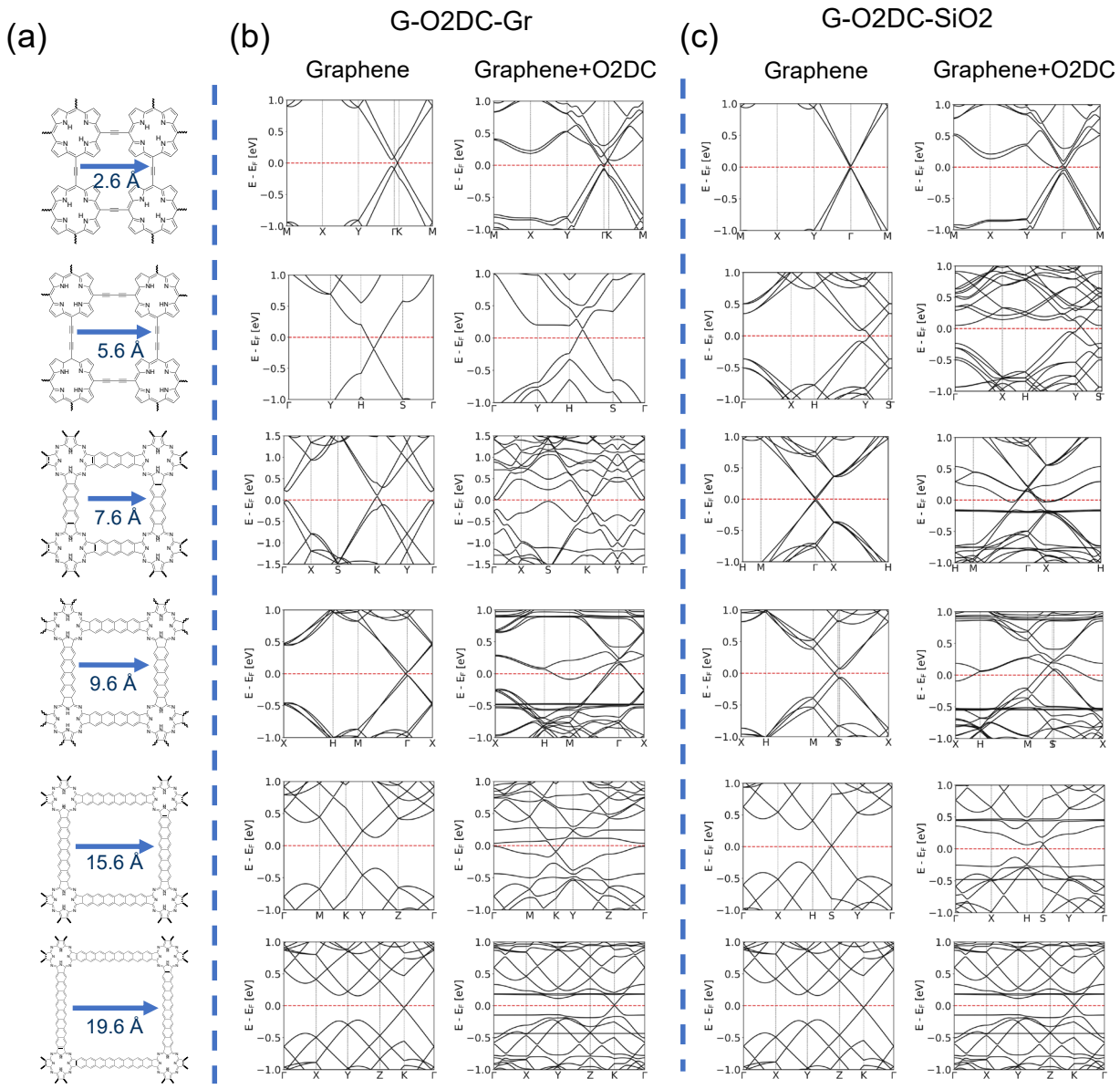

Figure S11. Band structures of sole graphene and graphene + O2DC moiety in G-O2DC-substrates (Gr and SiO_2) structures for studied O2DCs with square lattice.

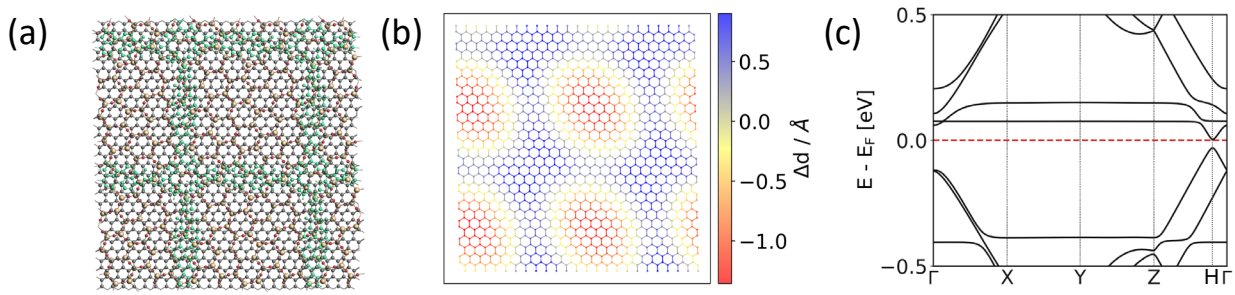

Figure S12. Example of influence of artificial strain on corrugation of graphene and its band structure. (a) G-O2DC-SiO_2 structure from a 2D rectangular polyimide O2DC. (b) Deformation analysis of graphene layer. (c) Band structure of G-O2DC moiety. Distortion that does not align with the shape of the pore from used O2DC can be seen clearly from (b), and a band gap is opened artificially.

Table S1. Band gap (meV) of studied configurations of **h1** to **h4** with substrates Gr/SiO_2. The rotational angles between graphene and O2DC are shown.

	h1 (18.9°)	h2 (0.0°)	h3 (23.0°)	h4 (25.1°)	h4 (8.0°)
G-O2DC-Gr	1.8	3.6	2.1	4.4	2.6
G-O2DC-SiO_2	0.8	5.6	1.8	8.6	2.0

Table S2. Band gap (meV) of studied configurations of **s1** to **s6** with substrates Gr/SiO_2. The rotational angles between graphene and O2DC are shown.

	s1 (0.0°)	s2 (9.9°)	s3 (13.8°)	s4 (5.5°)	s5 (34.2°)	s6 (27.0°)	s6 (21.5°)
G-O2DC-Gr	2.9	1.5	1.4	6.0	4.1	12.1	12.1
G-O2DC-SiO_2	5.2	3.0	1.0	3.5	6.6	11.4	8.2